Reorganization and polarization of the meiotic bouquet-stage cell can be uncoupled from telomere clustering

Carrie R. Cowan[1], Peter M. Carlton[2] and W. Zacheus Cande[1,2,*]

[1]Department of Plant and Microbial Biology and [2] Department of Molecular and Cell Biology, University of California – Berkeley, Berkeley, CA 94720-3200, USA

*Author for correspondence (e-mail: zcande@uclink4.berkeley.edu)

Summary

Striking cellular reorganizations mark homologous pairing during meiotic prophase. We address the interdependence of chromosomal and cellular polarization during meiotic telomere clustering, the defining feature of the bouquet stage, by examining nuclear positioning and microtubule and nuclear pore reorganization. Polarization of meiotic cellular architecture was coincident with telomere clustering: microtubules were focused on the nuclear surface opposite the telomere cluster, the nucleus was positioned eccentrically in the cell such that the telomeres faced the direction of nuclear displacement and nuclear pores were clustered in a single region of the nuclear surface opposite the telomeres. Treatment of pre-bouquet stage cells with colchicine inhibited telomere clustering.

Asymmetric nuclear positioning and nuclear pore clustering were normal in the presence of unclustered telomeres resulting from colchicine treatment. Nuclear pores were positioned normally with respect to the cell cortex in the absence of telomere clustering, indicating that telomere positioning is not required for polarization. This work provides evidence of meiotic cell polarization and suggests that telomeres may be positioned relative to an asymmetry present in the cell at the time of bouquet formation.

Key words: Bouquet, Telomere clustering, Meiosis, Nuclear pore clustering, Cell polarity

Introduction

Formation of the telomere cluster, the defining feature of the bouquet stage, is one mechanism by which chromosomes are brought into proximity in the meiotic prophase nucleus (Cowan et al., 2001; Scherthan, 2000; Zickler and Kleckner, 1998). Telomeres aggregate on a small region of the nuclear envelope coincident with chromosome pairing. Meiotic cells undergo cellular as well as nuclear reorganization during the bouquet stage (Zickler and Kleckner, 1998) and thus present a unique system to explore questions of intra- and extranuclear organization.

The meiotic telomere cluster is often compared to another example of chromosome polarization present in many cell types, the Rabl organization (Cowan et al., 2001). The Rabl organization results from persistence of the chromosome configuration brought about by spindle forces during mitosis; decondensed interphase chromosomes retain their anaphase arrangement. The consequence of this organization in metacentric organisms, including rye, is the formation of a nuclear axis, with telomeres defining one pole (i.e. the telomere pole) and the centromeres determining the opposite pole. The meiotic telomere cluster may be a remnant of the Rabl organization (Zickler and Kleckner, 1998); whether bouquet stage and Rabl telomere poles are similarly oriented with respect to cytoplasmic organelles is not known. As the

nucleus reforms during telophase, the centromeres are adjacent to the centrosome left over from the previous cell division. By contrast, during the bouquet stage, the centrosome in animal and yeast cells is adjacent to the telomere cluster. This suggests that the telomere cluster may have an altered orientation relative to the pre-existing cell axis when compared with polarized Rabl telomeres in a pre-meiotic cell.

Possible extra-chromosomal influences on telomere position during the bouquet stage have been extensively noted (Zickler and Kleckner, 1998). In animal and fungal cells, there is a marked proximity between the clustered telomeres and the microtubule organizing center (MTOC; centrosome and spindle pole body, respectively) during the bouquet stage (Buchner, 1910; Trelles-Sticken et al., 1999; Wilson, 1925; Zickler and Kleckner, 1998). Mitochondria are asymmetrically distributed in meiotic cells; the mitochondria aggregate adjacent to the nucleus, near the region of telomere clustering (Wilson, 1925). A 'mitochondria cloud' has been observed in the animals (al-Mukhtar and Webb, 1971; Church, 1976; Holm and Rasmussen, 1980; Moens, 1969; Rasmussen, 1976; Tourte et al., 1981) and plants (Hiraoka and Fuchikawa, 1993) in which it has been investigated, suggesting that it may be intimately tied to telomere clustering. In addition, many plants exhibit clustering of plastids near the bouquet-stage nucleus (Hiraoka, 1949a; Hiraoka, 1949b; Hiraoka and Fuchikawa,

1993; Rodkiewicz et al., 1986); however, in *Equisetum*, the plastids occupy a position diametrically opposed to the mitochondria cloud (Hiraoka and Fuchikawa, 1993). Nuclear pores (NPs) appear to redistribute around the nuclear envelope when telomere clustering occurs (Zickler and Kleckner, 1998). NPs aggregate into several large regions, often located near the telomeres, although the immediate site of telomere-nuclear envelope contact is generally devoid of NPs (Church, 1976; Hiraoka and Fuchikawa, 1993; Holm, 1977; Scherthan et al., 2000). Nuclear displacement accompanies bouquet formation in a wide range of organisms, including representatives of both the plant and animal kingdoms (Hiraoka, 1952; Wilson, 1925).

The clustering of telomeres into a small area and the polarization of this cluster along an axis can be regarded as two distinct phenomena. In both cases, the mechanisms are unknown. Do telomeres respond to a pre-existing cue in the cell that defines the site of the telomere cluster or is the telomere cluster initially randomly oriented? Because of the telomere cluster's proximity to the MTOC during the bouquet stage in many organisms, the question is most often viewed from the perspective of the MTOC: does the centrosome act as a telomere attractant or do clustered telomeres recruit the centrosome? Higher plants do not have focused MTOCs, although most species investigated display telomere clustering. In plants, the nuclear envelope appears to organize cytoplasmic MTs during both the somatic (Baskin and Cande, 1990; Stoppin et al., 1994; Vantard et al., 1990; Zhang et al., 1990) and meiotic (Chan and Cande, 1998) cell cycles. Is there a relationship between the site of telomere clustering and cytoplasmic microtubule organization in plants?

The present study addresses the organizing principles behind telomere clustering. We are concerned with the fundamental question: does the position of the telomere cluster polarize the cell or is there pre-determined, telomere-independent polarity in the meiotic cell? Bouquet-stage rearrangements are not limited to telomere clustering; cytoplasmic microtubules (MTs), NPs and the nucleus change their distribution within the cell. NP, nuclear and telomeric positions exhibit polarization during the bouquet stage. We previously demonstrated that telomere clustering is sensitive to colchicine (Cowan and Cande, 2002), allowing us to determine the consequences of inhibition of telomere clustering on the establishment of bouquet-stage cell polarity. The polarization events we investigated, with the exception of telomere position relative to the cell axis, were unaffected by inhibition of telomere clustering. Our results suggest that polarization of the telomeres occurs in response to a spatial cue provided by the cell, and chromosomal polarity has no apparent influence on cellular polarity during the bouquet stage.

Materials and Methods

Growth of rye plants
Rye plants (*Secale cereale* cv. Blanco) were grown in the greenhouse or outdoors (Berkeley, CA). The time between harvest and culture time 0 was less than 1 hour. Only the pedicellate floret was used in all experiments.

Anther culture
Upon removing anthers from the floret, the three anthers were longitudinally cut down the connective tissue joining the locules, giving rise to six anther halves. Upon bisecting an anther, the two halves were immediately placed into culture medium. Anther culture was performed as described elsewhere (Cowan and Cande, 2002).

Colchicine treatment
Colchicine (Sigma) exerted inhibitory effects after 3 hours of treatment; all experiments discussed were performed for a minimum of 12 hours. Complete (100% of meiotic cells) inhibition of telomere clustering was found with 75 µM colchicine and higher (Cowan and Cande, 2002). 75 µM colchicine, however, did not appear to cause complete depolymerization of cytoplasmic MTs, as judged by tubulin immunofluorescence (data not shown). 250 µM colchicine was used in experiments examining nuclear displacement, as this concentration resulted in a more complete depolymerization of cytoplasmic MTs, on the basis of tubulin immunofluorescence. All media contained 1% DMSO.

Fluorescent in situ hybridization (FISH)
Meiocytes and associated cells were embedded in 5% acrylamide polymerized between two coverslips. The FISH protocol was based on that of Bass et al. (Bass et al., 1997), as described previously (Cowan and Cande, 2002). Telomeres were detected using a probe for the telomere repeat (CCCTAAACCCTAAACCCTAAACCCTAAA) with either 5′ Cy5 or Texas Red (Genset).

Immunofluorescence
Meiocytes and associated cells were embedded in 5% acrylamide polymerized between two coverslips. Cell walls were digested with 1.5% β-glucuronidase (from *Helix pomatia*, Sigma) in 1×PBS at 36°C for 15 minutes for MT localization and for 1 hour for NP localization. Coverslips were washed thoroughly with 1×PBS. Primary antibody was applied in 1×PBS and incubated at room temperature overnight. Coverslips were washed in 1×PBS. The secondary antibody was applied in 1×PBS and incubated overnight at room temperature. Coverslips were washed in 1× PBS. Chromatin was stained with 3 µg/ml DAPI, and samples were mounted in glycerol.

Microtubules
Fixation was performed as described previously (Chan and Cande, 1998) using a monoclonal antibody against sea urchin α-tubulin (a gift of D. Asai, Purdue University) at 1:500 dilution. The primary antibody was visualized with Alexa-488-conjugated goat anti-mouse IgG (Molecular Probes) at 1:50 dilution.

Nuclear pores
Anthers were fixed in 4% paraformaldehyde in 1× buffer A for 15 minutes at room temperature. NPs were detected using a commercial monoclonal antibody against rat liver NP proteins (mAb 414; Covance) at 1:250 dilution. mAb414 recognized a major band of approximately 68 kDa protein on western blots, as well as minor bands at 93 and 29 kDa (data not shown). The primary antibody was visualized with either rhodamine-conjugated donkey anti-mouse IgG (Jackson Immunochemicals) at 1:75 dilution or FITC-conjugated goat anti-mouse IgG (Cappel) at 1:50 dilution; both secondary antibodies gave similar results.

Microscopy
Images were acquired with an Applied Precision DeltaVision microscope system equipped with an Olympus IX70 inverted microscope. A 40× 1.35 NA UApo oil immersion lens was used for
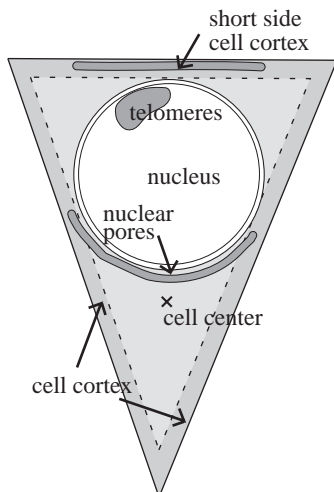
Fig. 1. A diagram of a bouquet-stage meiotic rye cell indicating the cellular components used for assessing polarity. Terms are defined in Materials and Methods. Details of individual measurements are given in Figs 4 and 5 and Fig. 8C.

all experiments. Cells were imaged in three dimensions (xyz); z-axis sections were collected at 0.2 μm spacing. Images were deconvolved using a standard conservative algorithm (Chen et al., 1995). Over 100 cells were examined for each treatment, time point and/or localization, although only a subset was used for quantitative analyses (described in the text).

Definition of terms and quantification of cell polarity

Several cellular structures were used to assess polarization of the rye meiotic cell and are summarized in Fig. 1. The cell cortex refers to the periphery of the cell but is not restricted to the plasma membrane. The short side cell cortex was defined by the tendency of rye meiotic cells to approximate isosceles triangles in shape and thus have two long sides and one short side. Telomeres were marked by the associated subtelomeric heterochromatic regions, as detected by intense DAPI staining. The nuclear volume was defined by the region occupying DAPI-stained chromatin, and, likewise, the nuclear periphery was determined by the outermost chromatin staining. Nuclear pores were detected using an antibody directed against a component of the nuclear pore complex, as discussed in the text. The cell center was calculated by finding the center of cell perimeter models.

Models of nuclei were created using the DeltaVision/softWoRx 3DModel program. The nuclear periphery was modeled on the outer edge of DAPI-stained chromatin. NP-containing regions were modeled according to mAb414 staining. The telomere position was modeled from heterochromatin-detected telomeres by picking the regions where heterochromatin represented the outermost DAPI signal. The subset of the cell cortex corresponding to the region bounded by tangents to the nucleus, approximately perpendicular to the cell cortex (see Fig. 4B) was modeled from MT or NP staining. MTs clearly delimited the cell boundary; NP staining was specific for the nuclear periphery so we relied on cellular background to find the cell cortex (data not shown).

3DModel data was imported into MATLAB (version 5.1.0.420, The MathWorks, Inc.) for quantitative analyses. The percentage of the nuclear surface occupied by NPs was calculated by binning nuclear periphery and NP models to 3×3×3 blocks and taking the ratio of overlapping blocks to total nuclear periphery blocks. Object centers were found by calculating the mean of the 3D object models. Random

angles were calculated between two random points in a sphere generated as follows: the azimuth was determined by a uniform random distribution of points between 0 and 2π; the elevation was calculated by the inverse sine of random points between –1 and 1. The angle measurements are not influenced by the radial position and thus the radius was maintained at 1.

Sample means are described plus/minus the standard deviation. Means were assessed for significant differences at 99% confidence ($P<0.01$) using an unequal variance Student's *t*-test. Distance and angle distributions are presented as box-whisker plots. The distribution values are divided into four quartiles, such that the first quartile contains 0-25% of the samples, the second quartile contains 25-50% of the samples, the third quartile contains 50-75 percent of the samples and the fourth quartile contains 75-100% of the samples. The median of the samples determines the boundary between the second and third quartiles. The quartiles are depicted as follows: the first quartile (0-25th percentage) corresponds to the bottom-most vertical single line; the second (25-50th percentage) and third (50-75th percentage) quartiles are contained within a box; the median is the horizontal line through the box and represents the boundary between the second and third quartiles; and the fourth quartile (75-100th percentage) corresponds to the upper-most vertical single line.

To ensure that our assignment of the short side cell cortex in colchicine-treated cells matched that of control cells, we calculated the cell center to cell cortex angle: the angle created between the cell center, the center of the nucleus and the center of the short side cell cortex. The cell center to cell cortex angle did not differ significantly between control and the 250 μM colchicine-treated cells (control, 151°±18°, $n=14$; colchicine-treated, 131°±35°, $n=10$).

Results

Rye heterochromatin accurately marks telomere position

Rye (*Secale cereale* cv. Blanco) was chosen to investigate meiotic reorganization for four reasons: the meiotic stage of rye can be easily identified through its chromatin morphology; it has long been used for meiotic research (Darlington, 1933); it has proved amenable to in vitro anther culture, unlike other grasses we tested; and rye chromosomes contain large blocks of heterochromatin in the subtelomeric region of each chromosome (Lima de Faria, 1952), allowing for the easy identification of telomeres by DAPI staining.

Since it is technically challenging to perform indirect immunofluoresence and FISH on the same cell population, in all experiments using indirect immunofluoresence, we used
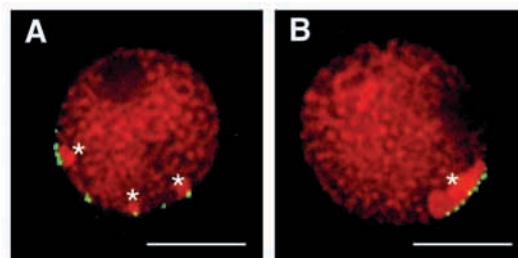

Fig. 2. Rye heterochromatin as an indicator of telomere distribution. Single z-sections of early meiotic prophase nuclei are shown. Telomeres (green) were detected by FISH. Chromatin (red) was stained with DAPI. Heterochromatin is visible as intensely staining DAPI regions (indicated with *). (A) Dispersed telomeres prior to the bouquet. Five of the eight FISH signals in this section are associated with heterochromatin. (B) Clustered telomeres during the bouquet. A single heterochromatic region is evident. Bar, 10 μm.

subtelomeric heterochromatin to monitor telomere positions. Rye heterochromatin was an accurate indicator of telomere position, and the extent of telomere clustering could be judged by heterochromatin distribution. Using FISH on the telomere repeat, we established that the large heterochromatic blocks in rye, revealed as intensely stained DAPI regions, were exclusively associated with telomere FISH signals. In pre-bouquet stage meiotic cells, when telomeres were dispersed, we were consistently able to recognize spatially distinct heterochromatin blocks (Fig. 2A), minimally representing one quarter of the telomere FISH signals (data not shown). Some heterochromatic regions appeared to represent more than one chromosome end, as indicated by multiple associated telomere signals (Fig. 2A). Fully clustered telomeres in the bouquet stage were visible as one large mass of heterochromatin associated with all telomere signals (Fig. 2B). In post-bouquet-stage nuclei, chromatin condensation masked the appearance of the subtelomeric heterochromatin; chromosome ends appeared to be similar to the rest of the chromatin. We were able to identify post-bouquet meiotic cells by chromosome morphology; they were confirmed using FISH, which marked the dispersed telomeres (data not shown).

Rearrangement of the microtubule cytoskeleton coincides with telomere clustering

We wished to know if there was a higher density of cytoplasmic MTs near the site of the telomere cluster in rye, as is seen in animal and fungal cells. In early meiotic prophase, cortical and randomly oriented cytoplasmic MTs were apparent (Fig. 3A). The cell shape was generally triangular and the nuclear position in the cell ranged from central to eccentric. In Fig. 1, we present a diagram of a rye meiocyte in the bouquet stage and show the cellular components used for assessing changes in cell polarity. The terms in the diagram are also defined in the Materials and Methods. During the bouquet stage, identified by the aggregated telomeric heterochromatin, the majority of MTs were focused toward the nucleus. Roughly two thirds of the nuclear surface was occupied with these focused MTs (Fig. 3B); fewer MTs were observed near the clustered telomeres. Bouquet-stage cells had a pronounced triangular shape. Nuclei appeared maximally eccentric in bouquet-stage cells and telomeres faced the cell cortex towards which nuclear displacement had occurred. After bouquet dissolution, MTs were still associated with a similar portion of the nuclear surface but now extended uniformly into the cytoplasm (Fig. 3C). Meiotic cells no longer appeared triangular but had assumed a rounded shape.

Telomeres are polarized relative to the cell during the bouquet stage

Bouquet-stage nuclei of rye appeared to be asymmetrically positioned in the cell, and the telomere cluster was oriented in the direction of displacement, away from the majority of MTs and the larger cytoplasmic volume (Fig. 3B). To quantify the polarization of the nuclear position within the cell, we calculated the distance between the center of the cell and the center of the nucleus (cell center-nucleus distance) in pre-bouquet, bouquet and post-bouquet cells (Fig. 4A). Distances were standardized to the nuclear radius. The mean cell center-nucleus distance was largest during the bouquet stage, significantly greater than both pre- and post-bouquet distances, confirming that the visibly eccentric nuclear position coincided with clustered telomeres. The cell center-nucleus distance values exhibited a wide range during all stages, perhaps because our calculations did not take into account cell size and shape.

The asymmetric nuclear positioning at the bouquet stage appeared to result from displacement along the long axis of the meiotic cell. In general, the mid-plane of meiotic cells approximated an isosceles triangle. As described above, the fully clustered telomeres faced the cell cortex towards which nuclear displacement had occurred and thus the short side of the triangular cell. Although we did not investigate cell shape intensively, we were able to identify the short side cell cortex in most cells, which provided a marker of cell asymmetry. To
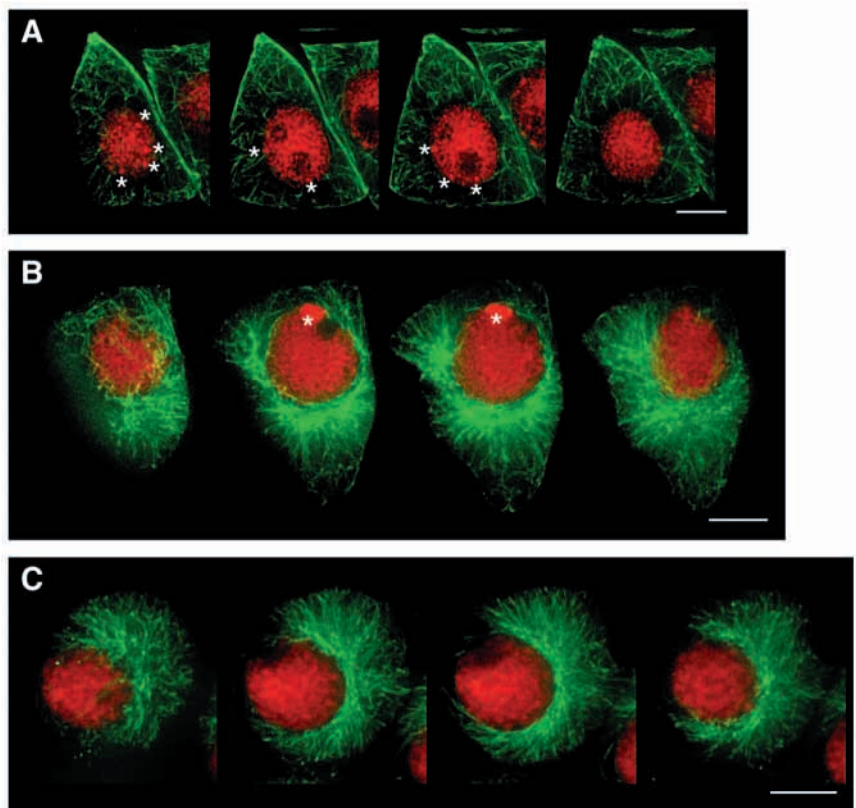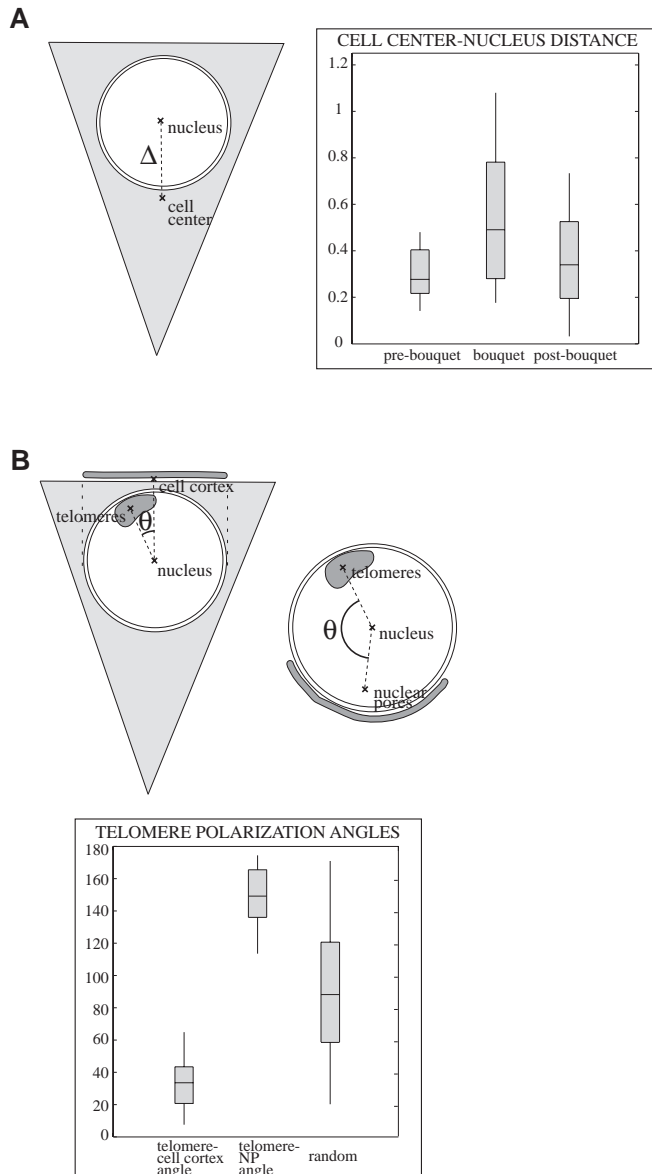

Fig. 3. Cytoplasmic MT distribution during early meiotic prophase. To convey the 3D architecture of the cell, the data corresponding to the entire cellular volume (approximately 100 z-sections) were divided into quarters, and each quarter was projected into a single image (Bass et al., 1997). The resulting images are displayed sequentially. MTs (green) were detected with an antibody against α-tubulin. Chromatin (red) was stained with DAPI, and telomere positions were inferred from the telomeric heterochromatin (a subset indicated with *) in (A) and (B). (A) Pre-bouquet, (B) bouquet and (C) post-bouquet. Bars, 10 μm.

A

B

Fig. 4. (A) The position of the nucleus in early meiotic prophase. The cell center-nucleus distance is the distance between the center of the cell and the center of the nucleus. A diagram of the distance (Δ) used to quantify nuclear displacement is shown. A box-whisker plot of the cell center-nucleus distance in pre-bouquet (n=12), bouquet (n=14) and post-bouquet (n=18) cells is shown. Distances were standardized to the nuclear radius. The cell center-nucleus distance units are based on the nuclear radius, such that the radius equals 1 unit. (B) Bouquet-stage polarization. The telomere-cell cortex angle is the angle created between the center of the telomeric heterochromatin, center of the nucleus and the center of the cell cortex. The cell cortex is the subset of the short side cell cortex bounded by tangents perpendicular to the nucleus. The telomere-NP angle is the angle created between the center of the telomeric heterochromatin, the center of the nucleus and the center of the NP-containing region. Diagrams of the telomere-cell cortex and telomere-NP angles used to determine bouquet-stage polarization are shown. Angles are indicated by θ. A box-whisker plot of telomere-cell cortex (n=22) and telomere-NP (n=30) angles in bouquet-stage cells is shown. Bouquet-stage angles were compared with the distribution of random angles between two points in a sphere through the center of the sphere (n=50). In both (A) and (B), the box represents the second and third quartiles, the horizontal line through the box is the median and whiskers extend to the range (see also Materials and Methods).
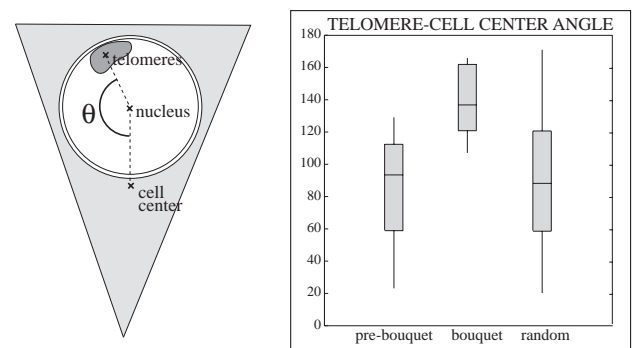

Fig. 5. Telomere position relative to the cell in Rabl or bouquet organizations. The telomere-cell angle is the angle created between the center of the telomeric heterochromatin, the center of the nucleus and the cell center. A diagram of the telomere-cell angle used to calculate telomere position within the cell is shown. The angle is indicated by θ. A box-whisker plot (as in Fig. 4) of the telomere-cell angles for pre-bouquet (n=11) and bouquet (n=14) stage cells, compared with the distribution of random angles in a sphere (n=50), is shown.

evaluate the position of the telomere cluster relative to the short side cell cortex, we calculated the angle created between the centers of the short side cell cortex, nucleus and telomeres (telomere–cell-cortex angle; Fig. 4B). The telomere-cell cortex angle had a mean value of 33°±14° (n=22), which was significantly different from the distribution of random angles through the center of the sphere (90°±41°, n=50). The telomere cluster therefore occupies a specific cellular position relative to the short side cell cortex.

Meiotic telomere polarization relative to the cell axis is not predicted by the Rabl organization

Rye exhibits a strong Rabl organization in pre-bouquet cells, with telomeres located in one hemisphere of the nucleus (Fig. 2A) (Dong and Jiang, 1998; Mikhailova et al., 2001). Given our finding that telomeres were polarized with respect to the cell during the bouquet (telomere-cell cortex angle, Fig. 4B),

we next asked whether the polarized Rabl telomeres were specifically positioned relative to the cell axis and whether they can be used to predict the position of the bouquet-stage telomere pole. In pre-bouquet cells, it was difficult to assign a short side cell cortex, as cells were closer in shape to equilateral triangles (Fig. 3A). To compare telomere positioning with the cell axis in pre-bouquet and bouquet-stage cells, the angle created between the centers of the cell, nucleus and telomeres (telomere-cell center angle) was calculated and compared with the distribution of random angles (Fig. 5). The telomere–cell-center angle of pre-bouquet cells was similar to the random distribution (pre-bouquet, 86°±33°, n=11; random, 90°±41°, n=50; Fig. 5), in contrast to the bouquet-stage telomere–cell-

center angle (bouquet, 140°±20°, n=14; Fig. 5), suggesting a constrained polarization of telomeres relative to the cell during the bouquet stage. The random orientation of telomeres in pre-bouquet cells suggests that bouquet-stage telomere polarization relative to the cell axis is not predicted by the cellular position of the polarized Rabl telomeres in the pre-bouquet cell.

Nuclear pores and telomeres are diametrically opposed during the bouquet stage

The highly polarized rye bouquet-stage nucleus provided a unique opportunity to investigate the spatial relationship between the NPs and clustered telomeres. Although components of the NP complex in plants have not been well characterized, we found that an antibody raised against rat liver NP proteins [mAb414 (Davis and Blobel, 1987)] was a useful marker in rye nuclei. The antibody was specific for the nuclear periphery of both somatic and meiotic cells and appeared to localize outside the chromatin staining, as judged by immuno-

Fig. 6. Nuclear pore reorganization during early meiotic prophase. Sequential z-axis projections of meiotic cells, as described in Fig. 3. NPs (green) were immunolocalized using an antibody against nuclear pore proteins (mAb414). Chromatin (red) was stained with DAPI, and telomere positions were inferred by the telomeric heterochromatin (a subset indicated with *) in (A) and (B). (A) Pre-bouquet, (B) bouquet and (C) post-bouquet. Bars, 10 μm.

fluorescence (Fig. 6). Variable nucleolar staining (Fig. 6) and pre-bouquet nucleoplasmic background (Fig. 6A) occurred with the secondary antibody alone (data not shown).

NPs were distributed uniformly around the nuclear surface during early meiotic prophase, and telomeric heterochromatin was dispersed throughout the nuclear periphery (Fig. 6A). When telomeres were fully clustered, as evidenced by the aggregated heterochromatin, NPs were also clustered (Fig. 6B). The NP cluster lay adjacent to the bulk of the cytoplasm (data not shown); the telomere cluster was diametrically opposed to the NPs. NPs occupied 37±7% (n=22) of the nuclear surface during the bouquet stage, in contrast to coverage of the entire nuclear surface in pre-bouquet cells. After telomeres had dispersed from the bouquet, NPs associated with regions of chromatin-nuclear envelope contact; chromatin-free regions of the nuclear periphery did not show NPs (Fig. 6C). At this stage the nuclear envelope is still intact.

To quantify the polarization of the telomere cluster relative to NPs during the bouquet, we calculated the angle created between the centers of the NP-containing region, nucleus and telomeres (Fig. 4B). The telomere-NP angle exhibited little variance among experiments (147°±18°, n=30). We compared this value to the distribution of random angles in a sphere and found the random distribution (90°±41°, n=50) to be significantly different from the observed mean telomere-NP angle (Fig. 4B). The standard deviation of the bouquet-stage telomere-NP angles was less than the standard deviation of random angles, indicating that the bouquet-stage organization of telomeres and NPs was spatially constrained.
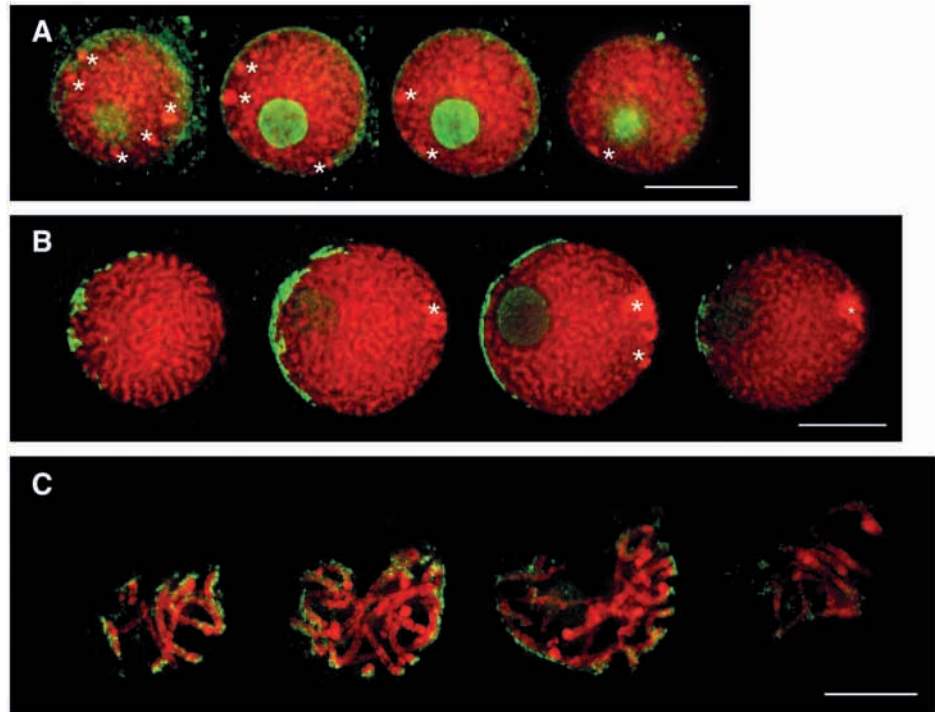
Asymmetric nuclear positioning can occur without telomere clustering

Our finding that telomere clustering could be inhibited experimentally by colchicine (Cowan and Cande, 2002) allowed us to investigate the influence of chromosomal organization on cellular architecture. Early meiotic prophase anthers were treated with 250 μM colchicine. In time 0 meiotic cells, telomeres were dispersed, MTs were distributed randomly in the cytoplasm, and nuclei were predominantly central in the cell (Fig. 7A, time 0). After 8-14 hours in culture, untreated cells reached the bouquet stage: telomeres were completely clustered, the nucleus was located eccentrically in the cell, the telomere cluster faced the cell cortex, and MTs were distributed asymmetrically around the nuclear surface (Fig. 7A, control). Colchicine-treated cells exhibited scattered telomeres, and cytoplasmic MTs were not evident (Fig. 7A, 250 μM colchicine). Nuclear displacement, however, occurred despite the failure of telomere clustering, and mean cell center-nucleus distances in control and colchicine-treated cells were similar (Fig. 7B; Table 1).

We investigated the spatial relationship between the unclustered telomeres and the short side cell cortex in colchicine-treated cells. The telomere–cell-cortex angle (see Fig. 4B) differed significantly in colchicine-treated and control cells (Table 1). The distribution of telomere positions relative to the cell cortex in colchicine-treated cells was shifted towards a random distribution (Fig. 7C). Inhibition of telomere clustering by colchicine resulted in telomere misorientation relative to the cell cortex.
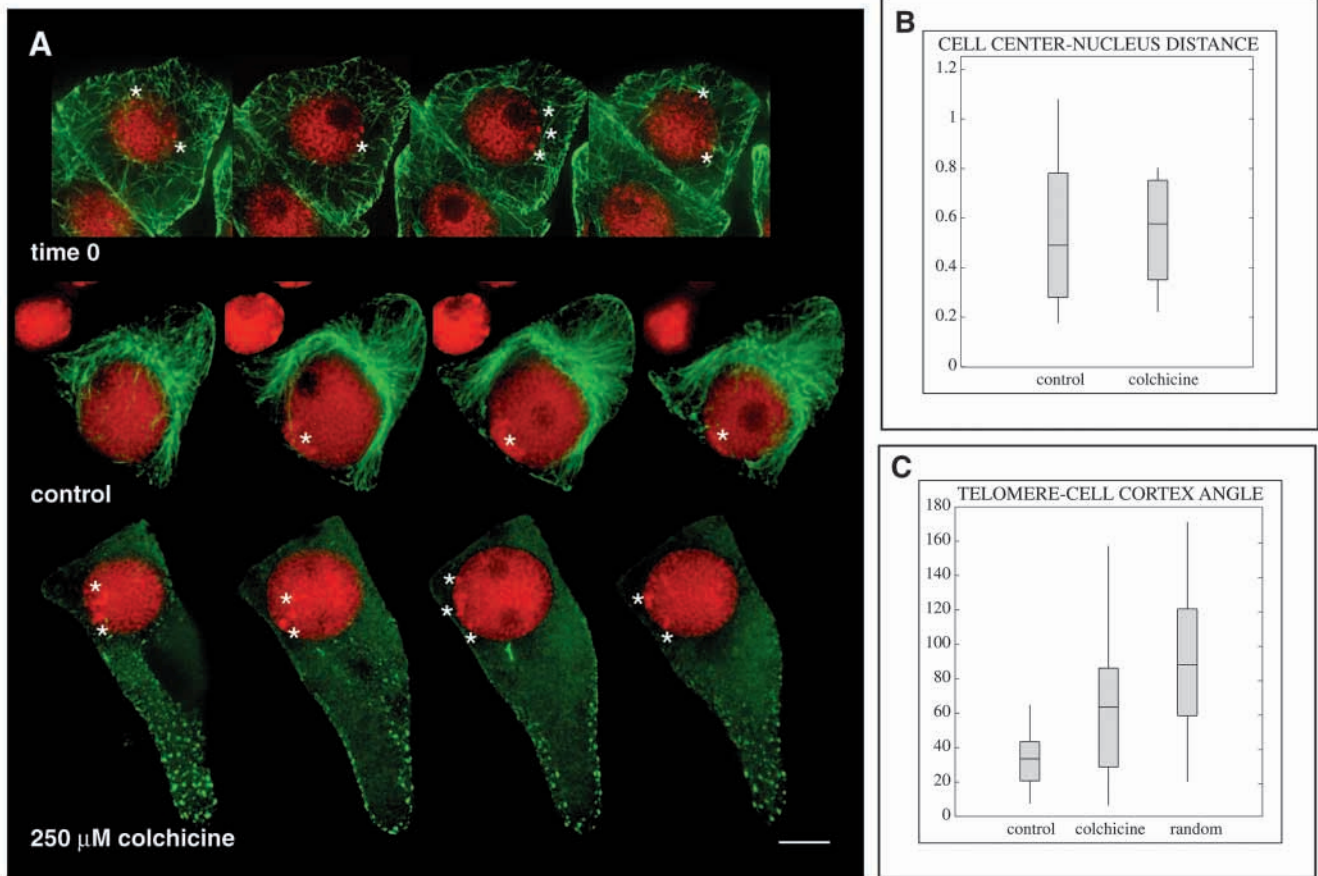
Fig. 7. Nuclear displacement and telomere positioning in colchicine-treated bouquet-stage cells. (A) Sequential z-axis projections of meiotic cells, as described in Fig. 3. Control and 250 μM colchicine-treated anthers were cultured for 14 hours. MTs (green) were detected with an antibody against α-tubulin. Chromatin (red) was stained with DAPI, and telomere positions were inferred from the telomeric heterochromatin (a subset indicated with *). Bar, 10 μm. (B) Nuclear positioning in colchicine-treated cells. A box-whisker plot (as in Fig. 4) of telomere-cell center distance, as calculated in Fig. 4, for control (*n*=14) and 250 μM colchicine-treated (*n*=10) cells is shown. The cell center-nucleus distance units are standardized to the nuclear radius, such that the radius equals 1 unit. (C) Telomere polarization relative to the cell cortex in colchicine-treated cells. A box-whisker plot of telomere-cell cortex angle, as described in Fig. 6, for control (*n*=22) and 100 μM and 250 μM colchicine-treated (grouped together; *n*=22) cells, compared with the distribution of random angles in a sphere (*n*=50).

Nuclear pore reorganization and polarization can occur independently of telomere clustering

We wished to determine whether telomere clustering is a prerequisite for NP reorganization or whether telomere-generated asymmetry is involved in positioning the clustered NPs. Early meiotic prophase anthers were treated with 100 μM colchicine. In time 0 nuclei, telomeres were dispersed and NPs were uniformly distributed around the nuclear periphery (Fig. 8A, time 0). After a sufficient culture period, a single telomere cluster was observed in control nuclei, whereas in colchicine-treated cells telomeres were dispersed in the nuclear periphery. NP distribution, however, was identical in colchicine-treated and control nuclei; NPs were located in a single region of the nuclear periphery (Fig. 8A, control and 100 μM colchicine). NPs occupied similar percentages of the nuclear surface in colchicine-treated and control cells (Fig. 8B; Table 1).

In control nuclei, NPs were located strictly opposite the telomere cluster. However, in colchicine-treated nuclei, the

Table 1. Bouquet stage polarization

Polarization	Control	Colchicine-treated	Significantly different (*P*<0.01)
Cell center-nucleus distance	0.55±0.28	0.54±0.20	–
Telomere-cell cortex angle	33°±14°	64°±41°	+
Telomere-NP angle	147°±18°	119°±41°	+
NP-cell cortex angle	158°±11°	144°±14°	–
NP percentage	37±7	42±14	–

Polarization of cellular architecture during the bouquet stage and the effect of colchicine on polarization. Mean values plus or minus the standard deviation are given for the asymmetries examined. The cell center-nucleus distance units are based on the nuclear radius, such that the radius equals 1 unit. The distributions of control and colchicine-treated data were assessed for difference using an unequal variance Student's *t*-test; hypotheses were tested at 99% confidence (*P*<0.01). + indicates that the distributions were significantly different, – indicates that the distributions were not significantly different. For comparison, the distribution of random angles between two points within a sphere through the center of the sphere exhibited a mean of 90°±41° (*n*=50).
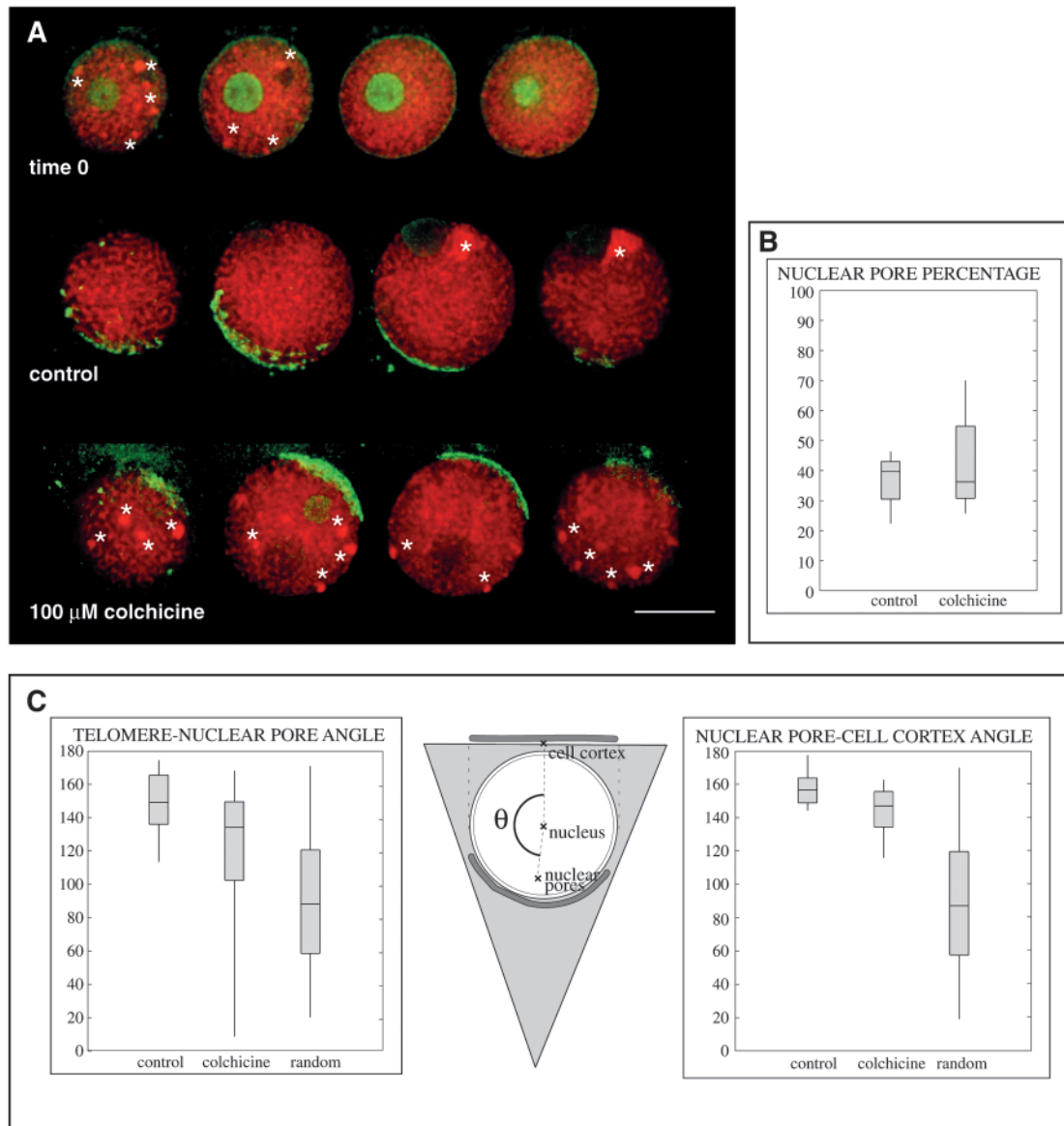
Fig. 8. Nuclear pore redistribution and polarization in colchicine-treated bouquet-stage cells. (A) Sequential z-axis projections of meiotic nuclei, as described in Fig. 3. Control and 100 μM colchicine-treated anthers were cultured for 12 hours. NPs (green) were immunolocalized using an antibody against nuclear pore complex proteins (mAb414). Chromatin (red) was stained with DAPI. Positions of telomeres were inferred from heterochromatin (a subset indicated with *). Bar, 10 μm. (B) NP clustering in colchicine-treated cells. A box-whisker plot of the percentage of the nuclear surface occupied by NPs in control ($n=22$) and 100 μM colchicine-treated ($n=22$) nuclei. (C) Polarization of NPs in colchicine-treated cells. A box-whisker plot (as in Fig. 4) of telomere-NP angles (as in Fig. 6) in control ($n=30$) and 100 μM colchicine-treated ($n=34$) nuclei, compared with the distribution of random angles in a sphere ($n=50$). The NP-cell cortex angle is the angle created between the center of the NP-containing region, the center of the nucleus and the center of the cell cortex (Fig. 4B). A diagram of NP-cell cortex angle is shown; the angle is indicated by θ. A box-whisker plot of NP-cell cortex angle in control ($n=8$) and 100 μM colchicine-treated ($n=12$) cells is shown. Also shown is the distribution of random angles in a sphere ($n=50$).

position of telomeres relative to the NPs was unconstrained. Partial overlaps of telomeres and NPs were observed occasionally. The NP-telomere angle (Fig. 4B) in colchicine-treated cells was significantly different from that in control cells and exhibited greater variation (Fig. 8C; Table 1). These findings, however, were difficult to interpret, owing to the lack of polarization of unclustered telomeres; the telomere–cell-cortex angle differed significantly in control and colchicine-treated cells (Fig. 7C; Table 1).

In an attempt to resolve whether the induced loss of NP-telomere polarity was a result of the mislocalization of telomeres alone or of both NPs and telomeres, we examined the positioning of the NP cluster relative to the cell cortex towards which nuclear displacement had occurred. NP position in the cell was assessed by determining the angle between the centers of the NP-containing region, nucleus and cell cortex (Fig. 8C). The mean NP–cell-cortex angle was not significantly different in control and colchicine-treated cells, and both these

angles were different from random expectations (Fig. 8C; Table 1), suggesting that NP position was not affected by the inhibition of telomere clustering.

Discussion

Several cellular reorganizations take place as telomeres cluster in rye, resulting in polarization of the bouquet-stage meiotic cell. The nucleus is moved to an eccentric position within the cell, the telomeres become oriented in the direction of nuclear displacement, cytoplasmic MTs are concentrated near the nuclear envelope opposite the region occupied by the telomeres and NPs cluster diametrically opposite the telomeres and cell cortex. A common axis underlies the organization of all these polarized components, suggesting a common polarization event. These aspects of meiotic cellular organization were not dependent on telomere clustering.

The use of colchicine provided important insights into the hierarchy of cellular polarization in the meiotic cell, although numerous questions arise from its effect on telomere clustering. The concentrations of colchicine used in these experiments (100 and 250 µM) had different effects on cytoplasmic MTs, as judged by tubulin immunofluorescence (data not shown). Telomere clustering, however, was unambiguously inhibited. Furthermore, other MT-depolymerizing drugs do not affect telomere clustering (Cowan and Cande, 2002). The focus of this discussion is on the interdependence of telomere clustering and cellular organization during the bouquet stage. Colchicine's mode of action in inhibiting telomere clustering is the subject of an accompanying paper, pp. 3749-3753.

Animal and fungal bouquet-stage cells show a clear proximity between the clustered telomeres and the MTOC (Buchner, 1910; Trelles-Sticken et al., 1999; Wilson, 1925; Zickler and Kleckner, 1998). The majority of cytoplasmic MTs in rye meiotic cells were focused toward the nuclear envelope, but their highest density was away from the position of the clustered telomeres. Although MT organization during early meiotic prophase in plants has not been previously investigated, MTOC activity during the bouquet stage appears to be favored in regions of the nuclear envelope not associated with the telomeres. In *Saccharomyces cerevisiae*, approximately one fifth of bouquet-stage nuclei exhibit clustered telomeres that are not associated with the spindle pole body (Trelles-Sticken et al., 1999). Thus positioning of telomeres in close proximity to the MTOC may not be a requirement for successful telomere clustering but rather may be evidence of an overall bouquet-stage cell polarity.

During the bouquet stage, the region of the nuclear envelope that had the highest density of MTs faced away from the short side cell cortex towards the bulk of the cytoplasm. Likewise, the nucleus was displaced to the region of the cell containing the largest volume of cytoplasm. The polarization of MT distribution on the nuclear envelope and nuclear position may be related by indirect means, for instance, a possible preference of both the nucleus and nuclear envelope MTOCs to be associated with organelles that are more highly represented in the bulk cytoplasm. The nuclear pores also exhibited a tendency to face away from the short side cell cortex toward the cell center during the bouquet stage. However, clustered telomeres were distinctly located away from the bulk of the cytoplasm during the bouquet, in close association with the short side cell cortex (Fig. 1).

Telomeres and NPs underwent two reorganizations: clustering and polarization. Numerous hypotheses have been proposed regarding the role of telomere clustering (Zickler and Kleckner, 1998), including the juxtaposition of homologous chromosomes, synaptonemal complex installation and initiation of recombination. NP clustering, by contrast, may be an indirect consequence of the requirement for telomere motility on the nuclear envelope (Scherthan et al., 2000). Why the telomere and NP clusters are specifically positioned in the meiotic cell is an intriguing question, and their localization perhaps suggests a more active role for the NP cluster in bouquet-stage events.

NP clustering during meiosis may reflect an overall reorganization of the nuclear envelope/lamina. Elimination of the single nuclear lamin in *Caenorhabditis elegans* using RNA-mediated interference results in NP clustering (Liu et al., 2000); likewise, NP clustering occurs in *Drosophila melanogaster* lamin Dm$_0$ mutants (Lenz-Boehme et al., 1997). These data suggest that the 'default' organization of NPs is to be clustered and that distribution of NPs throughout the nuclear envelope requires structural components, the lamins. It is possible that a reorganization of the nuclear lamina is a prerequisite for telomere motility.

The strict polarization of telomeres and NPs relative to each other as well as to the cell axis requires communication of positional information. Two models can be considered: first, cell polarity or NP position dictates telomere polarization. Alternatively, telomere positioning dictates NP position and cell polarity. We found that inhibition of telomere clustering did not affect either NP positioning relative to the cell axis or nuclear displacement toward the cell cortex, suggesting that clustered telomeres do not determine NP or cell polarization. Additionally, pre-bouquet telomeres were randomly oriented with respect to the cell axis. Thus, we can rule out the possibility that polarization of unclustered telomeres owing to the Rabl configuration is what determines the later axis of bouquet stage cell polarity. Cell shape was asymmetric in pre-meiotic cells (data not shown), suggesting that polarization cues may be present before the onset of meiotic prophase. Evidence from *Xenopus* (al-Mukhtar and Webb, 1971; Tourte et al., 1981) and locusts (Moens, 1969) indicates that meiotic cellular asymmetry exists prior to meiosis: mitochondria are positioned to one side of the nucleus as early as pre-meiotic interphase. It has been proposed that in mice and wheat (Riley and Flavell, 1977), the transition from a mitotic to meiotic cell cycle may occur during the several cell divisions preceding meiotic prophase; thus, cell polarity may be established well in advance of meiotic prophase.

Our analyses of the cellular and nuclear rearrangements, which occur in early meiotic prophase, reveal that extensive polarization of the cell as well as the chromosomes exists during the bouquet stage. Telomere clustering represents only one example of bouquet-stage polarity, and we have found that meiotic cell polarization can occur independently of telomere clustering. Thus, an understanding of the mechanism of formation of the telomere cluster must begin with an understanding of the origin of polarity in the meiotic cell as a whole.

members of the Cande lab for helpful comments concerning the manuscript.

References

al-Mukhtar, K. A. and Webb, A. C. (1971). An ultrastructural study of primordial germ cells, oogonia and early oocytes in *Xenopus laevis*. *J. Embryol. Exp. Morphol.* **26**, 195-217.

Baskin, T. I. and Cande, W. Z. (1990). The structure and function of the mitotic spindle in flowering plants. *Annu. Rev. Plant Physiol. Plant Mol. Biol.* **41**, 277-315.

Bass, H. W., Marshall, W. F., Sedat, J. W., Agard, D. A. and Cande, W. Z. (1997). Telomeres cluster de novo before the initiation of synapsis: A three-dimensional spatial analysis of telomere positions before and during meiotic prophase. *J. Cell Biol.* **137**, 5-18.

Buchner, P. (1910). Von den Beziehungen zwischen Centriol und Bukettstadium. *Arch. Zellforsch.* **5**, 215-228.

Chan, A. and Cande, W. Z. (1998). Maize meiotic spindles assemble around chromatin and do not require paired chromosomes. *J. Cell Sci.* **111**, 3507-3515.

Chen, H., Swedlow, J. R., Grote, M. A., Sedat, J. W. and Agard, D. A. (1995). The collection, processing, and display of digital three-dimensional images of biological specimens. In *Handbook of Biological Confocal Microscopy* (ed. J. B. Pawley), pp. 197-210. New York: Plenum Press.

Church, K. (1976). Arrangement of chromosome ends and axial core formation during early meiotic prophase in the male grasshopper *Brachystola magna* by 3D, E.M. reconstruction. *Chromosoma* **58**, 365-376.

Cowan, C. R., Carlton, P. M. and Cande, W. Z. (2001). The polar arrangement of telomere in interphase and meiosis. Rabl organization and the bouquet. *Plant Physiol.* **125**, 532-538.

Darlington, C. D. (1933). The origin and behaviour of chiasmata. VIII. Secale cereale (n, 8). *Cytologia (Tokyo)* **4**, 444-452.

Davis, L. I. and Blobel, G. (1987). Nuclear pore complex contains a family of glycoproteins that includes p62: glycosylation through a previously unidentified cellular pathway. *Proc. Natl. Acad. Sci. USA* **84**, 7552-7556.

Dong, F. and Jiang, J. (1998). Non-Rabl patterns of centromere and telomere distribution in the interphase nuclei of plant cells. *Chromosome Res.* **6**, 551-558.

Hiraoka, T. (1949a). Observational and experimental studies of meiosis with special reference to the bouquet stage. I. Cell polarity in the bouquet stage as revealed by the behaviour of plastids. *Bot. Mag. Tokyo* **62**, 19-23.

Hiraoka, T. (1949b). Observational and experimental studies of meiosis with special reference to the bouquet stage. II. Cell polarity in the bouquet stage as revealed by the behaviour of amyloplasts and fat granules. *Bot. Mag. Tokyo* **62**, 121-125.

Hiraoka, T. (1952). Observational and experimental studies of meiosis with special reference to the bouquet stage. XIV. Some considerations on a probable mechanism of the bouquet formation. *Cytologia (Tokyo)* **17**, 292-299.

Hiraoka, T. and Fuchikawa, Y. (1993). An electronmicroscopic and morphometric analysis on the cell polarity in the synaptic stage of meiosis. *Cytologia (Tokyo)* **58**, 77-84.

Holm, P. B. (1977). Three-dimensional reconstruction of chromosome pairing during the zygotene stage of meiosis in *Lilium longiflorum* (Thunb.) *Carlsberg Res. Commun.* **42**, 103-151.

Holm, P. B. and Rasmussen, S. W. (1980). Chromosome pairing, recombination nodules and chiasma formation in diploid Bombyx males. *Carlsberg Res. Commun.* **45**, 483-548.

Lenz-Boehme, B., Wismar, J., Fuchs, S., Reifegerste, R., Buchner, E., Betz, H. and Schmitt, B. (1997). Insertional mutational of the *Drosophila* nuclear lamin Dm$_0$ gene results in defective nuclear envelopes, clustering of nuclear pore complexes, and accumulation of annulate lamellae. *J. Cell Biol.* **137**, 1001-1016.

Lima de Faria, A. (1952). Chromomere analysis of the chromosome complement of rye. *Chromosoma* **5**, 1-68.

Liu, J., Ben-Shahar, T. R., Riemer, D., Treinin, M., Spann, P., Weber, K., Fire, A. and Gruenbaum, Y. (2000). Essential roles for *Caenorhabditis elegans* lamin gene in nuclear organization, cell cycle progression, and spatial organization of nuclear pore complexes. *Mol. Biol. Cell* **11**, 3937-3947.

Mikhailova, E., Sosnikhina, S., Kirillova, G., Tikholiz, O., Smirnov, V., Jones, R. and Jenkins, G. (2001). Nuclear dispositions of subtelomeric and pericentromeric chromosomal domains during meiosis in asynaptic mutants of rye (Secale cereale L.). *J. Cell Sci.* **114**, 1875-1882.

Moens, P. B. (1969). The fine structure of meiotic chromosome polarization and pairing in *Locusta migratoria* spermatocytes. *Chromosoma* **28**, 1-25.

Rasmussen, S. W. (1976). The meiotic prophase in *Bombyx mori* females analyzed by three dimensional reconstructions of synaptonemal complexes. *Chromosoma* **54**, 245-293.

Riley, R. and Flavell, R. B. (1977). A first view of the meiotic process. *Phil. Trans. R. Soc. Lond. B Biol. Sci.* **277**, 191-199.

Rodkiewicz, B., Bednara, J., Mostowska, A., Duda, E. and Stobiecka, H. (1986). The change in disposition of plastids and mitochondria during microsporogenesis and sporogenesis in some higher plants. *Acta Bot. Neerl.* **35**, 209-215.

Scherthan, H., Jerratsch, M., Li, B. B., Smith, S., Hulten, M., Lock, T. and de Lange, T. (2000). Mammalian meiotic telomeres: Protein composition and redistribution in relation to nuclear pores. *Mol. Biol. Cell* **11**, 4189-4203.

Stoppin, V., Vantard, M., Schmit, A.-C. and Lambert, A.-M. (1994). Isolated plant nuclei nucleate microtubule assembly: The nuclear surface in higher plants has centrosome-like activity. *Plant Cell* **6**, 1099-1106.

Tourte, M., Mignotte, F. and Mounolou, J.-C. (1981). Organization and replication activity of the mitochondrial mass of oogonia and previtellogenic oocytes in *Xenopus laevis*. *Dev. Growth Differ.* **23**, 9-21.

Trelles-Sticken, E., Loidl, J. and Scherthan, H. (1999). Bouquet formation in budding yeast: Initiation of recombination is not required for meiotic telomere clustering. *J. Cell Sci.* **112**, 651-658.

Vantard, M., Levilliers, N., Hill, A.-M., Adoutee, A. and Lambert, A.-M. (1990). Incorporation of Paramecium axonemal tubulin into higher plant cells reveals functional sites of microtubule assembly. *Proc. Natl. Acad. Sci. USA* **87**, 8825-8829.

Wilson, E. B. (1925). *The cell in development and heredity*. New York: Macmillan.

Zhang, D., Wadsworth, P. and Hepler, P. K. (1990). Microtubule dynamics in living dividing plant cells: confocal imaging of microinjected fluorescent brain tubulin. *Proc. Natl. Acad. Sci. USA* **87**, 8820-8824.

Zickler, D. and Kleckner, N. (1998). The leptotene-zygotene transition of meiosis. *Annu. Rev. Genet.* **32**, 619-697.